JOURNAL OF THERMOPHYSICS AND HEAT TRANSFER
Vol. 6, No. 4, Oct.–Dec. 1992

Correlation Transfer: Application of Radiative Transfer Solution Methods to Photon Correlation Problems

B. J. Ackerson,* R. L. Dougherty,† N. M. Reguigui,‡ and U. Nobbmann§
Oklahoma State University, Stillwater, Oklahoma 74078

A correlation transfer equation is developed for multiple scattering applications, and is solved for the field correlation function that is measured by photon correlation experiments. Radiative transport solution techniques are applied, because there is a formal similarity between the two theories. Small correlation delay time, isotropic scattering and optically thick media approximations are made to compare with experimental results and to derive diffusive wave spectroscopy theory, the currently accepted photon correlation theory for optically dense media. The "deposition length" problem in diffusive wave theory for the backscattering geometry is investigated in detail. To improve the comparison between theoretical and experimental results, it is concluded that the isotropic scattering assumption must be relaxed. Unlike diffusive wave theory, relaxation of the three aforementioned assumptions is straightforward in the correlation transfer theory by adapting existing radiative transport solution methods and will be the subject of subsequent investigations.

Nomenclature

A = cross-sectional area (perpendicular to illumination) of a target volume containing one potential scatterer; it is proportional to the inverse of the particle number density to the two-thirds power
a = multiplicative constant used in approximating E_1, [Eq. (47)]
B = basic radiative transfer source function
b = exponential constant used in approximating E_1, [Eq. (47)]
C = unnormalized intensity correlation function
c = speed of light
D_0 = dilute solution (single scattering) diffusion constant for Brownian motion
D_1 = radiative transfer diffusion constant
d = diameter of particles suspended in a fluid
E = electric field
E^* = complex conjugate of electric field
E_1 = exponential integral, [Eq. (46)]
F_1 = constant used in approximate correlation transfer solution, [Eq. (49)]
F_2 = constant used in approximate correlation transfer solution, [Eq. (49)]
G = Green's function solution of diffusion equation
G^m = unnormalized multiple scattering field correlation function—any direction
G_1^{m+} = one-dimensional multiple scattering correlation function—transmitted
G_1^{m-} = one-dimensional multiple scattering correlation function—backscattered
G_0^+ = magnitude of "incident" correlation
G^s = unnormalized single scattering field correlation function
g = normalized electromagnetic field correlation function
g^1 = normalized single scattering electric field correlation function
g^{1*} = complex conjugate of g^1
g^m = normalized multiple scattering field correlation function—any direction
g^{m+} = normalized multiple scattering field correlation function—transmitted
g^{m-} = normalized multiple scattering field correlation function—backscattered
$h_i^{\pm}$ = coefficients used in the approximate one-dimensional solution for the correlation function, [Eqs. (50–52)]
I = intensity
$\langle I \rangle^m$ = ensemble average of intensity for multiple scattering
I_0 = magnitude of incident intensity
i = summation counter and $\sqrt{-1}$
$J(s)$ = probability of having a multiple scattering path of length s
j = summation counter
$\boldsymbol{k}$ = wavevector
k_B = Boltzmann's constant
$\boldsymbol{k}_i$ = ith wavevector in a multiple scattering path, where i indicates the ith scattering event
$\boldsymbol{k}_{i,i-1}$ = difference between the wavevector $\boldsymbol{k}_i$ and the wavevector $\boldsymbol{k}_{i-1}$
$\boldsymbol{k}_0$ = incident wavevector
$\boldsymbol{k}_1$ = scattered wavevector
L = physical thickness of medium
$\bar{L}$ = optical thickness of medium, L/l
$\bar{L}_e$ = effective equivalent optical thickness of medium for RT solutions, $\bar{L}/\bar{\omega}$
l = mean free path
l^* = effective mean free path for equivalent isotropic scattering
N = number of suspended particles in a given target volume
N_j = number of scattering events in path j
n = index of refraction and summation counter
$\hat{\mathbf{n}}$ = outward normal to a surface
$p(j)$ = number of multiple scattering paths having j scattering events
Q = number of possible paths in a multiple scattering medium
$\mathbf{r}$ = physical three-dimensional location

Received June 7, 1991; presented as Paper 91-1433 at the AIAA 26th Thermophysics Conference, Honolulu, HI, June 24–26, 1991; revision received Oct. 21, 1991; accepted for publication Oct. 24, 1991.

*Professor, Physics Department, 145 Phys. Sci.
†Associate Professor, School of Mechanical and Aerospace Engineering, EN 218. Member AIAA.
‡Research Assistant, School of Mechanical and Aerospace Engineering, EN 218.
§Research Assistant, Physics Department, 145 Phys. Sci.

R = $(1 - \tilde{\omega}_a/b)$
S_g = correlation source term
S_{g0} = magnitude of correlation source term
S_I = intensity source term
s = length of a multiple scattering path
T = temperature
t = time
U = density of diffusing photons in radiative transfer problem
V = intermediate function in time-dependent correlation transfer solution, [Eq. (31)]
$\tilde{V}$ = angular average of V
W = intermediate function in time-dependent correlation transfer solution, [Eq. (30)]
$\tilde{W}$ = angular average of W
$w_i^{\pm}$ = coefficients used in the approximate one-dimensional solution for the correlation function, [Eqs. (53–55)]
X = Chandrasekhar's source function at the upper boundary of a finite medium exposed to collimated incident intensity
x = dummy variable of integration
Y = Chandrasekhar's source function at the lower boundary of a finite medium exposed to collimated incident intensity
z = optical coordinate
$z^{\pm}$ = optical coordinate which is either equal to zero or to $\tilde{L}_e$
z_0 = physical depth at which a laser beam must be deposited
$\tilde{z}$ = physical coordinate
α = constant depending on experimental detector setup
β = coefficient specifying the distribution of deposition depths for incident radiation
γ = signal-to-noise ratio (factor)
ζ = a decay coefficient
η = viscosity of solvent
Θ = angle between incident and scattered intensity (or wavevector), measured in the scattering plane
θ = polar angle
κ = absorption coefficient
λ = wavelength of electromagnetic waves in a vacuum
μ = cosine of the polar angle
μ_0 = μ corresponding to the polar angle of the incident radiation
ν = Laplace transform variable
ρ = number density of particles
σ = macroscopic scattering coefficient, $1/l$
σ^* = microscopic scattering cross section of a particle
τ = correlation delay time
τ_0 = correlation delay time constant, $1/D_0k_0^2$
Φ = scattering phase function or form factor
ϕ = azimuthal angle
ϕ_0 = azimuthal angle of the incident radiation
$\boldsymbol{\omega}$ = Fourier transform variable
$\tilde{\omega}$ = single scattering albedo
$\boldsymbol{\Omega}$ = angular direction of intensity propagation
$\boldsymbol{\Omega}_0$ = angular direction of propagation of incident intensity
$d\Omega$ = differential solid angles, $\sin\theta\, d\theta\, d\phi$

Introduction

PHOTON correlation or dynamic light scattering techniques have proven highly useful in characterizing fluid/particle suspension properties such as particle diameter, fluid viscosity and diffusion constants.[1-4] However, for accurate characterization, the suspensions must be very dilute (optically thin) so that multiple scattering is minimal and the single scattering Born approximation[1] may be employed to interpret the data. For more concentrated suspensions (increasing optical thickness), theoretical corrections have been made to account for multiple scattering.[5,6] These theories are highly complex, and are difficult to extrapolate to arbitrary orders of multiple scattering. Thus, they are best applied to lower orders of multiple scattering. Experimentally, multiple scattering effects in optically thicker media may be suppressed by cross-correlation techniques,[7-9] but experimental run times increase as the singly scattered intensity decreases with increasing turbidity.

Recently, the highly multiple scattering limit (optically thick) has been examined experimentally and theoretically with success.[10-12] This study of the time dependence of intensity fluctuations has been termed diffusive wave spectroscopy (DWS), because use is made of the fact that the radiation executes a diffusive propagation (random walk) in passage through the scattering medium. The first of these recent studies examined the intensity correlation function in backscattering to study the phenomenon of weak localization.[13,14] It was further extended to transmission studies and a more quantitative theory was developed. This has been followed by recent studies at very short correlation times[15] (allowing the study of very small particle displacements) and pulse shape studies.[16]

In this paper, we develop and solve a correlation transfer (CT) equation, that is based on the intuition underlying the DWS theory. Because it assumes ballistic transfer of light, CT should be more generally applicable than DWS. Furthermore, it is formally similar to radiative transfer (RT) theory. It should be as accurate as RT in modelling multiple scattering, and known RT methods may be adapted to solve the CT equation.

Because photon correlation methods may not be familiar to the reader, this topic is reviewed in both the single scattering and highly multiple scattering (DWS) limits in the Review section. In the Development section, the correlation transfer equation is presented with heuristic arguments justifying its form. Its relation to radiative transport and to single scattering are given. Small delay time, preaveraging, and large optical density assumptions are made to simplify and solve the CT equation in the DWS limit. The formal structure of the DWS theory is derived from this approximate CT equation, so solutions to the approximate equation should correspond to DWS solutions. Solutions are obtained using standard radiative transport methods. In the Discussion section, the exact numerical and approximate CT results are compared with corresponding DWS results. Special attention is given to the "deposition length" problem encountered in DWS, but not in CT, and we give arguments for the proper resolution of this problem. Finally, in the Conclusions section, we deduce that the assumptions made by DWS are too restrictive, leading to the disagreement between theory and experiment in backscattering geometries. We give a heuristic argument explaining that the preaveraging assumption is responsible for the disagreement between theory and experiment. CT results which do not assume preaveraging will be the topic of a future publication.

Review

Single Scattering Photon Correlation Theory

We begin our development with a review of the single scattering theory for an optically dilute suspension of independent, noninteracting, diffusing particles. The suspension is illuminated by a plane electromagnetic wave having a wavevector $\boldsymbol{k}_0$ with magnitude $2\pi n/\lambda$, where λ is the wavelength of the incident radiation in a vacuum (Fig. 1), n is the refractive index of the solvent, and the direction of $\boldsymbol{k}_0$ is represented by $\boldsymbol{\Omega}'$. The intensity is detected at a large distance from the scattering volume, so the scattered wave approximates a plane wave with scattered wavevector $\boldsymbol{k}_1$ (and direction $\boldsymbol{\Omega}$). The momentum transferred in the scattering is proportional to $\boldsymbol{k} = \boldsymbol{k}_1 - \boldsymbol{k}_0$. For this quasi-elastic scattering, the momentum is related to the scattering angle Θ with respect

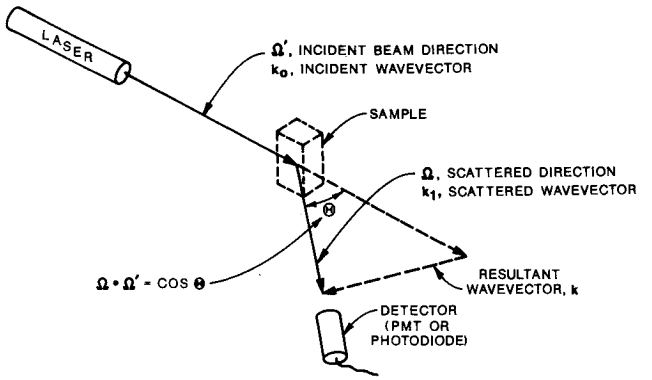

Fig. 1 Scattering geometry and notation.

to the incident beam direction by way of the relationship for the magnitude of the wavevector, $k = 4\pi n \sin(\Theta/2)/\lambda = 2k_0 \sin(\Theta/2)$, where $\cos(\Theta) = \mathbf{\Omega}' \cdot \mathbf{\Omega}$. Here, it is assumed that the wavelength does not change upon scattering.

The measurement of the average scattered intensity $\langle I(\mathbf{r}, \mathbf{\Omega}, t)\rangle$, is performed by ensemble averaging the instantaneous intensity $I(\mathbf{r}, \mathbf{\Omega}, t)$. For stationary or ergodic processes,[17] this may be replaced by a time average. This average intensity is proportional to the product of the scattered electric field $E(\mathbf{r}, \boldsymbol{k}, t)$ and its complex conjugate[18]:

$$\langle I(\mathbf{r}, \mathbf{\Omega}, t)\rangle = \alpha\langle E(\mathbf{r}, \boldsymbol{k}, t)E^*(\mathbf{r}, \boldsymbol{k}, t)\rangle \tag{1}$$

The proportionality constant (α) in Eq. (1) depends upon the detection area and other physical characteristics of the detection system. The instantaneous intensity at the detector depends on the interference pattern produced by scattering from the instantaneous configuration of particles and may deviate far from the average value. When using visible laser light to illuminate a colloidal sample, this interference is often observed as a "speckle pattern," which may be seen when the pattern is projected on a nearby plane surface. Theoretically, the instantaneous scattered electric field may be represented as a summation of the singly scattered fields from each of the particles in the scattering volume ($E = \Sigma E_j$). Then the instantaneous intensity is comprised of two types of terms (Eq. (2a)), those involving the same particle, and those involving different particles. The interference terms involving different particles give rise to fluctuations about the average scattered intensity. On the average, the mutual interference terms of the scattered electric field from different independent particles are zero. The only surviving contribution from these interference terms yields an average scattered intensity that is proportional to the intensity scattered by single particles as follows:

$$\langle I(\mathbf{r}, \mathbf{\Omega}, t)\rangle = \alpha \sum_j^N \sum_m^N \langle E_j(\mathbf{r}, \boldsymbol{k}, t)E_m^*(\mathbf{r}, \boldsymbol{k}, t)\rangle \tag{2a}$$

$$= \alpha \sum_j^N \langle E_j(\mathbf{r}, \boldsymbol{k}, t)E_j^*(\mathbf{r}, \boldsymbol{k}, t)\rangle \tag{2b}$$

$$= \alpha N I_0 \sigma^* \Phi(\boldsymbol{k})/A \tag{2c}$$

Here, I_0 is the magnitude of the incident intensity, and the total electric field at the detector is written in terms of a sum of single scatterings from each of the N particles in the scattering volume. A is the cross-sectional area (normal to the illumination) which is proportional to the sample volume per particle raised to the two-thirds power. In this case, all particles are assumed identical, having the same scattering cross section (σ^*) and producing the same phase function Φ (or single particle form factor). The Eq. (2c) form for the average scattering intensity is well known and used to determine particle structure, radius of gyration, and other related properties.[19]

As the suspended particle configuration changes in time, the instantaneous scattered intensity will fluctuate as the interference pattern evolves. A correlation function (g) is used to relate the fluctuating intensity to electric field fluctuations. This function correlates the electric field time history to that same field where the time history has been shifted by a delay time τ:

$$g(\mathbf{r}, \boldsymbol{k}, \tau) = \langle E(\mathbf{r}, \boldsymbol{k}, t)E^*(\mathbf{r}, \boldsymbol{k}, t + \tau)\rangle/$$

$$\langle E(\mathbf{r}, \boldsymbol{k}, t)E^*(\mathbf{r}, \boldsymbol{k}, t)\rangle \tag{3}$$

For uniform illumination of the scattering volume and for single scattering, the correlation function (and electric field) becomes independent of location, $\mathbf{r}$, and g is designated by g^1. Equation (3) can then be represented by a summation over the single scattering by all particles.

The power spectrum of the scattered intensity may be measured and is directly proportional to the time Fourier transform of the electric field correlation function,[1] g^1. Rather than the power spectrum, it is more common to measure the intensity correlation function $C(\mathbf{r}, \boldsymbol{k}, \tau)$, that is defined as[20]

$$C(\mathbf{r}, \boldsymbol{k}, \tau) = \langle I(\mathbf{r}, \mathbf{\Omega}, t)I(\mathbf{r}, \mathbf{\Omega}, t + \tau)\rangle \tag{4}$$

For single scattering from N independent diffusing particles, the correlation function is independent of location, and the statistics of the scattered electric field are Gaussian. In this case, the intensity correlation function may be expressed in terms of the field correlation function. The averages may be carried out similar to the average scattered electric field discussed above. The cross terms between different particles again average zero, and the relation between the intensity correlation function $C(\boldsymbol{k}, \tau)$ and the [electric] field correlation g^1 is given by the Siegert relation[20,21]

$$C(\boldsymbol{k}, \tau) = \langle I(\mathbf{r}, \mathbf{\Omega}, t)\rangle^2[1 + g^1(\boldsymbol{k}, \tau)g^{1*}(\boldsymbol{k}, \tau)] \tag{5a}$$

which with Eq. (2c) becomes

$$= [\alpha N I_0 \sigma^* \Phi(\boldsymbol{k})/A]^2[1 + |g^1(\boldsymbol{k}, \tau)|^2] \tag{5b}$$

The single scattering field correlation function for monodisperse independent diffusing particles is given by[1,20]

$$g^1(\boldsymbol{k}, \tau) = \exp(-D_0 k^2 \tau)$$

$$= \exp[-2D_0 k_0^2 \tau(1 - \mathbf{\Omega} \cdot \mathbf{\Omega}')] \tag{6a}$$

$$\approx 1 - 2D_0 k_0^2 \tau(1 - \mathbf{\Omega} \cdot \mathbf{\Omega}'), \qquad \text{for } D_0 k_0^2 \tau \ll 1.0 \tag{6b}$$

where the relation $k^2 = 2(1 - \mathbf{\Omega} \cdot \mathbf{\Omega}')k_0^2$ has been used, and D_0 is the dilute solution diffusion constant. For spherical particles,[19] this diffusion constant is given by the Stokes-Einstein relation

$$D_0 = k_B T/(3\pi\eta d) \tag{7}$$

with η being the solvent viscosity and d being the particle diameter. In actual experiments, a signal-to-noise factor γ (≤ 0.8) multiplies the product of the field correlation functions within the intensity correlation equation (Eqs. (5a) and (5b)). This signal-to-noise factor results from the finite size of the scattering volume and detection surface.[22,23]

The previous results must be modified for dependent scattering, when the particles interact with one another and do not assume completely random configurations. The cross terms which averaged to zero for independent particles now give a contribution, but the results look formally similar to those for the independent particles.[2]

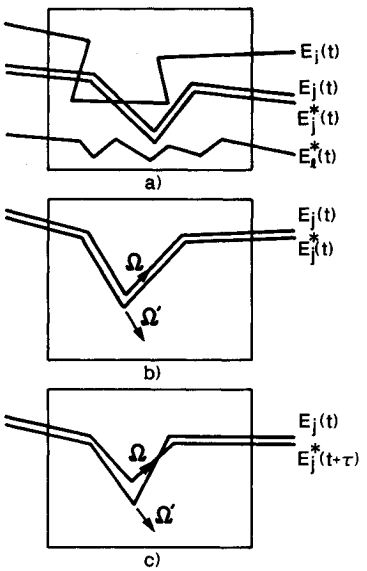

Fig. 2 DWS approach to determine the surviving scattered field interference terms.

Diffusive Wave Spectroscopy

In systems which are too concentrated for the single scattering approximations to remain valid, the methods of the previous section cannot be applied. Rather, the scattered field at the detector may be considered as a sum of electric fields, each representing one of the possible multiple scattering paths through the sample. In the limit of strong multiple scattering of the incident field, the polarization direction will become randomly distributed, and the scattered electric field direction becomes isotropically distributed on a length scale of order l^*—the effective transport mean free path.[12] Under these optically thick conditions, the light executes a random walk or diffuses through the medium. This is the domain of DWS.

Because the intensity is a product of multiply scattered fields, there results a number of terms in the formal expression for the intensity (Eq. (1)) which are products of fields representing different paths through the sample as represented in Fig. 2a. All of these terms contribute to the instantaneous scattered intensity at any time. However, those terms representing two different multiple scattering paths will average to zero upon forming the ensemble average over all positions of the independent particles. This happens because the different multiple scattering paths will represent different lengths and therefore different phases of the scattered wave at the detector. Since different paths will have at least one uncommon particle and that particle may be moved independently, the phase difference between the two multiply scattered fields in the field product term is arbitrary. The average of that field product term over this arbitrary phase is zero. Thus, the only terms which contribute to the ensemble average intensity are those that represent the same particles in each of the multiple scattering paths. It is also assumed in DWS theory that the multiple scattering path connecting the particles for each field must be identical to have a significant contribution to the average of the field product term. Thus, it is argued that the only important contributions to the intensity come from terms that represent the product of two fields, each of which represents the same multiple scattering path through the sample,[10] as represented in Fig. 2b. This is expressed formally as

$$\langle I(\mathbf{r}, \mathbf{\Omega}, t)\rangle^m = \alpha \sum_j^Q \sum_n^Q \langle E_j(\mathbf{r}, \boldsymbol{k}, t)E_n^*(\mathbf{r}, \boldsymbol{k}, t)\rangle \quad (8a)$$

$$= \alpha \sum_j^Q \langle E_j(\mathbf{r}, \boldsymbol{k}, t)E_j^*(\mathbf{r}, \boldsymbol{k}, t)\rangle \quad (8b)$$

$$= \sum_j^Q \langle I_j(\mathbf{r}, \mathbf{\Omega}, t)\rangle \quad (8c)$$

Here, the subscripts (n and j) on the field enumerate the different multiple scattering paths. In the special case of backscattering, these paths are counted twice because light enters and leaves both ends of these multiple scattering paths, giving rise to an enhanced backscattering effect termed "weak localization."[10] This diffraction effect is limited to within a few degrees of true backscattering and may be ignored for dynamic scattering measurements at larger backscattering angles (>3°). For this reason, we do not include this effect in the theory developed here.

Each term in the calculation of the average intensity in Eq. (8c) represents the transfer of intensity from particle to particle for a given multiple scattering path. If the individual scatterers are sufficiently well separated, then the single scattering result, $(\sigma^*/A)\Phi(\boldsymbol{k})$ (cf. Eq. (2c)), may be used to represent the transfer of intensity in each scattering event for independent or noninteracting particles. However, in this case, $\boldsymbol{k}$ must represent an intermediate scattered wavevector ($\boldsymbol{k}_{i,i-1}$), which is the difference between the new scattering wavevector ($\boldsymbol{k}_i$) and the previous scattering wavevector ($\boldsymbol{k}_{i-1}$) (where i refers to the ith scattering event) in the multiple scattering path.[10]

The previous argument also can be applied to the unnormalized version of Eq. (3) in order to find an expression for the unnormalized field correlation function (G^m) for independent diffusing particles

$$G^m(\boldsymbol{k}, \tau) = \langle E(\mathbf{r}, \boldsymbol{k}, t)E^*(\mathbf{r}, \boldsymbol{k}, t + \tau)\rangle$$

$$= \sum_j^Q \langle E_j(\mathbf{r}, \boldsymbol{k}, t)\, E_j^*(\mathbf{r}, \boldsymbol{k}, t + \tau)\rangle \quad (9a)$$

$$= I_0 \sum_j^Q \prod_i^{N_j} (\sigma^*/A)\Phi(\boldsymbol{k}_{i,i-1})\exp(-D_0 k_{i,i-1}^2 \tau) \quad (9b)$$

where N_j is the number of scattering events in path j. Equation (9a) assumes that terms including two different multiply scattered paths average to zero (see Figs. 2a and 2b). Then Eq. (9b) is a sum over all multiple scattering paths assuming that each scattering event may be represented using the single scattering results for independent particles as explained in the previous section on Single Scattering Photon Correlation Theory. The field correlation function produced by these significant paths decays to zero as the particles diffuse. This is caused by dephasing as the path lengths change relative to one another with increasing τ (Fig. 2c). A small time approximation is then made, allowing expansion of the exponent as in Eqs. (6) and an averaging (or integration) over all possible orientations of the intermediate scattered wavevector $\boldsymbol{k}_{i,i-1}$. This we refer to as "preaveraging," which, for small times and assuming isotropic scattering ($\Phi(\boldsymbol{k}_{i,i-1}) = 1.0$), may be expressed by the following summation of exponentials:

$$G^m(\boldsymbol{k}, \tau) = I_0 \sum_i^\infty p(i)(\sigma^*/A)^i \exp(-2i\tau/\tau_0) \quad (10)$$

where $\tau_0 = 1/D_0 k_0^2$, i is the number of scattering events, and $p(i)$ is the number of paths with i scattering events. This result may be approximated as an integral over $J(s)$, the probability of having a path with length s

$$G^m(\boldsymbol{k}, \tau) \approx I_0 \int_0^\infty J(s)\exp[-(2\tau/\tau_0)s/l^*]\, \mathrm{d}(s/l^*) \quad (11)$$

where the path length, s, is given by the product of the number of scattering events i and the effective mean free path length l^*; i.e., $s = il^*$. The effective mean free path, l^*, is used here instead of the mean free path, l, in order to account for anisotropic effects.[12] The G^m correlation function may be

normalized through division by $G^m(\boldsymbol{k}, \tau = 0)$ to yield

$$g^m(\boldsymbol{k}, \tau) = G^m(\boldsymbol{k}, \tau)/G^m(\boldsymbol{k}, \tau = 0)$$

$$\propto \int_0^\infty J(s)\exp[-(2\tau/\tau_0)s/l^*]\, ds \tag{12}$$

The function $J(s)$ is obtained for different geometries by the argument that each light path represents a "diffusive" random walk. Paths s, each of the same length, take the same amount of time ($t = s/c$) between entering, diffusing, and leaving the sample—due to the fact that the light travels with constant speed (c) between scattering collisions. Thus, we must solve a diffusion equation for the boundary conditions of illumination and loss, with the time between entry and exit of a photon being directly related to its path length in the sample. That diffusion equation is given by[12]

$$\frac{\partial U(\mathbf{r}, t)}{\partial t} = D_1 \nabla^2 U(\mathbf{r}, t) \tag{13}$$

where D_1 is the photon diffusion constant, $cl^*/3$, and $U(\mathbf{r}, t)$ is the density of the diffusing photons. $J(s)$ is proportional to $-\hat{\mathbf{n}}\cdot\nabla U(\mathbf{r}, t)$ at the surface point of interest, where $\hat{\mathbf{n}}$ is the outward normal at that surface point. The specific geometry and boundary conditions of interest must be supplied to solve Eq. (13).

Reference 12 gives the equations for backscattering and transmission based on the assumption of "depositing" a unit intensity at a physical depth z_0 within a one-dimensional planar medium of physical thickness L. This deposition depth (z_0) is a necessary assumption within this approximation because diffusion of light is only accomplished after several scatterings. Several scatterings are required in order for the light propagation to be considered random. However, the value of z_0 is not well defined, and must be estimated based on assumptions, such as a zero average photon flux into the sample medium at the physical boundary of the sample, giving $z_0 = 0.7104l^*$.[24,25] This value is approximate, indicating only that z_0/l^* should be near unity. However, the exact value of z_0/l^* is critical, particularly for accurate evaluation of backscattering. Since l^* is an effective path length, L/l^* and z_0/l^* may be considered optical locations in the backscattered and transmitted equations. Reference 12 solutions are presented as functions of these terms, and have been experimentally validated for small delay time, τ. For backscattering, the equation is

$$g^{m-}(\tau) = \frac{\sinh\left[\sqrt{\frac{6\tau}{\tau_0}}\left(\frac{L}{l^*} - \frac{z_0}{l^*}\right)\right] + \frac{2}{3}\sqrt{\frac{6\tau}{\tau_0}}\cosh\left[\sqrt{\frac{6\tau}{\tau_0}}\left(\frac{L}{l^*} - \frac{z_0}{l^*}\right)\right]}{\left(1 + \frac{8}{3}\frac{\tau}{\tau_0}\right)\sinh\left(\frac{L}{l^*}\sqrt{\frac{6\tau}{\tau_0}}\right) + \frac{4}{3}\sqrt{\frac{6\tau}{\tau_0}}\cosh\left(\frac{L}{l^*}\sqrt{\frac{6\tau}{\tau_0}}\right)} \tag{14}$$

which, for a sample of infinite thickness ($L \to \infty$), becomes

$$g^{m-}(\tau) = \frac{\exp[-(z_0/l^*)\sqrt{6\tau/\tau_0}]}{1 + \frac{2}{3}\sqrt{\frac{6\tau}{\tau_0}}} \tag{15}$$

and then for small τ/τ_0, becomes

$$g^{m-}(\tau) \approx \exp[-(z_0/l^* + 2/3)\sqrt{6\tau/\tau_0}] \tag{16}$$

For transmission, the Ref. 12 equations are

$$g^{m+}(\tau) = \frac{\frac{L + (4/3)l^*}{z_0 + (2/3)l^*}\left\{\sinh\left(\frac{z_0}{l^*}\sqrt{\frac{6\tau}{\tau_0}}\right) + \frac{2}{3}\sqrt{\frac{6\tau}{\tau_0}}\cosh\left(\frac{z_0}{l^*}\sqrt{\frac{6\tau}{\tau_0}}\right)\right\}}{\left(1 + \frac{8\tau}{3\tau_0}\right)\sinh\left(\frac{L}{l^*}\sqrt{\frac{6\tau}{\tau_0}}\right) + \frac{4}{3}\sqrt{\frac{6\tau}{\tau_0}}\cosh\left(\frac{L}{l^*}\sqrt{\frac{6\tau}{\tau_0}}\right)} \tag{17a}$$

$$\approx \frac{\left(\frac{L}{l^*} + \frac{4}{3}\right)\sqrt{\frac{6\tau}{\tau_0}}}{\left(1 + \frac{8\tau}{3\tau_0}\right)\sinh\left(\frac{L}{l^*}\sqrt{\frac{6\tau}{\tau_0}}\right) + \frac{4}{3}\sqrt{\frac{6\tau}{\tau_0}}\cosh\left(\frac{L}{l^*}\sqrt{\frac{6\tau}{\tau_0}}\right)}, \quad \tau/\tau_0 << 1.0 \tag{17b}$$

For large optical thickness, i.e., $L/l^* >> z_0/l^*$, and for small delay times, i.e., $L/l^*(6\tau/\tau_0)^{0.5} << 1.0$, Eqs. (14) and (17a) become

$$g^{m-}(\tau) = \exp[-4(L/l^*)(\tau/\tau_0)] \tag{18}$$

$$g^{m+}(\tau) = \exp[-(L/l^*)^2(\tau/\tau_0)] \tag{19}$$

Here, the + and − signs appended to g^m represent the forward and backward scattering directions for wavevector $\boldsymbol{k}$. Note that for backscattering, the limits $L \to \infty$ and $\tau \to 0$ lead to different results depending on the order in which they are executed. In Eqs. (15) and (16), the limit of infinite optical thickness, $L \to \infty$, is taken first. In Eqs. (17b), (18), and (19), the limit of small delay time, $\tau \to 0$, is taken first. For infinite optical thickness, only Eq. (15) applies, as shown by the solid line in Fig. 3. For any finite optical thickness, there exist times $(6\tau/\tau_0)^{0.5} << l^*/L$ for which Eqs. (18) and (19) apply, as can be inferred from the small delay time ranges in Figs. 3 and 4.

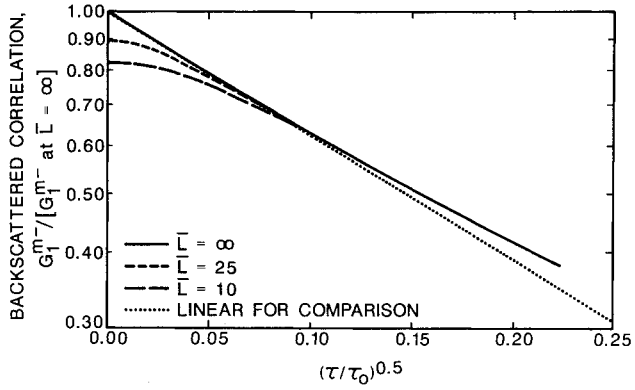

Fig. 3 Comparison of exact backscattered correlation as a function of the square root of delay time for various $\bar{L}$.

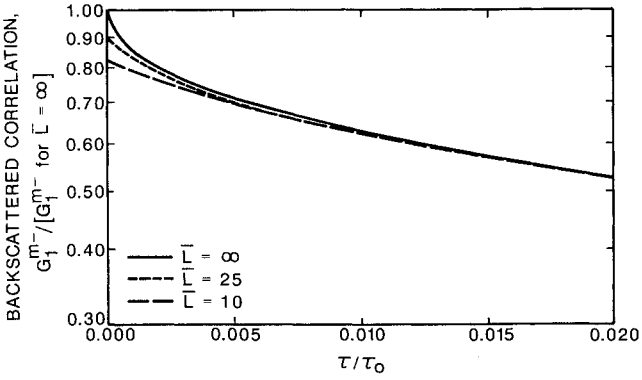

Fig. 4 Comparison of exact backscattered correlation as a function of the delay time for various $\bar{L}$.

Development

Correlation Equation

In the argument for the DWS result, no interference of electric fields is assumed between different multiple scattering paths on the average. These assumptions appear consistent with the viewpoint employed in developing a RT transport equation, where intensity is transferred from element to element in space, based on an energy conservation principle. In the derivation of such a transfer equation, interference between different multiple scattering paths is neglected on the average.[26]

The RT equation is an integro-differential equation given by[18]

$$(1/c)\partial\langle I(\mathbf{r}, \mathbf{\Omega}, t)\rangle/\partial t + \mathbf{\Omega}\cdot\nabla\langle I(\mathbf{r}, \mathbf{\Omega}, t)\rangle + \kappa\langle I(\mathbf{r},\mathbf{\Omega}, t)\rangle + \sigma\langle I(\mathbf{r}, \mathbf{\Omega}, t)\rangle = \langle S_I(\mathbf{r}, \mathbf{\Omega}, t)\rangle + (\sigma/4\pi)\int_{4\pi}\langle I(\mathbf{r}, \mathbf{\Omega}', t)\rangle\Phi(\mathbf{\Omega}, \mathbf{\Omega}')\,d\Omega' \quad (20)$$

This is an equation for the ensemble averaged intensity $\langle I(\mathbf{r}, \mathbf{\Omega}, t)\rangle$. Here, $d\Omega'$ represents the solid angle in the direction of propagation of light for a volume element located at position $\mathbf{r}$ in the sample at time t. The time derivative allows for the investigation of nonsteady processes or pulse propagation, where c is the speed of light in the medium. The spatial gradient term represents the change in intensity between different spatial locations. The next two terms account for absorption and scattering of the light out of the $\mathbf{\Omega}$ direction, respectively. Note that the scattering coefficient σ, is an inverse mean free path between scattering events, equal to $1/l$. The integral term represents scattering of radiation at $\mathbf{r}$ into the $\mathbf{\Omega}$ direction. Radiation is introduced into the system either by the source term in Eq. (20) ($S_I(\mathbf{r}, \mathbf{\Omega}, t)$) or through boundary conditions.

The proposed CT equation looks very similar to the previous RT equation, as follows:

$$(1/c)\partial G^m(\mathbf{r}, \mathbf{\Omega}, t, \tau)/\partial t + \mathbf{\Omega}\cdot\nabla G^m(\mathbf{r}, \mathbf{\Omega}, t, \tau) + \kappa G^m(\mathbf{r}, \mathbf{\Omega}, t, \tau) + \sigma G^m(\mathbf{r}, \mathbf{\Omega}, t, \tau) = S_g(\mathbf{r}, \mathbf{\Omega}, t) + (\sigma/4\pi)\int_{4\pi} G^m(\mathbf{r}, \mathbf{\Omega}', t, \tau)g^1(\mathbf{k}', \tau)\Phi(\mathbf{\Omega}, \mathbf{\Omega}')\,d\Omega' \quad (21)$$

where the wavevector $\mathbf{k}'$ is used to designate the wavevector difference between direction $\mathbf{\Omega}'$ and $\mathbf{\Omega}$ (Fig. 1 and Eqs. (6)), and $G^m(\mathbf{r}, \mathbf{\Omega}, t, \tau)$ is a time dependent designation for $G^m(\mathbf{k}, \tau)$.

Comparing Eq. (8b) with the $\tau = 0$ version of Eq. (9a) shows that the zero delay time correlation function is identical to the average intensity in the RT equation. Thus, we expect the CT equation to be identical to the RT equation at zero time delay. This is seen to be true by comparing Eq. (20) and the $\tau = 0$ version of Eq. (21). We assume implicitly that the speed of light is very large compared to the particle diffusive motion. Thus, the average field correlation function is realized essentially instantaneously for each value of τ. That is, particle positions may be considered frozen for each τ. For nonzero values of τ, small displacements of the particles from their initial positions decrease the correlation due to dephasing between the paths at t and $t + \tau$. As shown in Fig. 2c, these are still nearly the same paths, but they must be weighted differently due to the additional random phase introduced when the length of the path at t differs from the length at $t + \tau$.

By examining the correlation process in comparison to the radiative transfer process, we can arrive at the CT equation through appropriate modifications of the RT equation. Correlation is affected by the scattering process, as in single scattering, so that we need only consider modifying the scattering terms in the RT equation to fit the correlation process. Unlike energy, correlation is not conserved. This is due to the fact that correlation actually reduces with delay time τ. For this reason, the two scattering terms in the RT equation (the last terms on both sides of Eq. (20)) must be handled separately.

To understand the differences between the two terms, we again consider Figs. 2b and 2c. In both the RT process (Fig. 2b) and CT process (Fig. 2c), those paths which represent scattering out of the $\mathbf{\Omega}$ direction (the last term on the left sides of Eqs. (20) and (21)) give no further contribution to the intensity or correlation in that direction. There are other nonscattered paths or forward scattering paths, but their contributions are the same in both cases, because forward scattering produces no decay of field correlation functions (refer to Eq. (6a) for $\mathbf{\Omega} = \mathbf{\Omega}'$). Thus, this scattering term is the same for RT and for CT, producing the same fraction of scattered paths out of the $\mathbf{\Omega}$ direction in both cases.

It is another question to ask how much intensity or correlation is scattered into the direction $\mathbf{\Omega}$. In Fig. 2b, the amount of intensity transferred depends on the cross section and phase function (or form factor). For RT, what is scattered into the $\mathbf{\Omega}$ direction comes from the other directions $\mathbf{\Omega}'$ such that energy conservation is maintained. In Fig. 2c, the amount of correlation transferred depends on the cross section, the phase function (or form factor), and on the single particle field correlation function. Here we assume that the particles are sufficiently well separated to act as single independent scatterers. Thus, correlation may be scattered out of one direction, but is transferred less and less completely into the $\mathbf{\Omega}$ direction as τ increases and the single particle field correlation function decreases. The CT equation then takes the form given in Eq. (21). Reference 24 has derived a similar equation from a perturbation expansion in the first-order smoothing approximation for particles moving with uniform velocity. Evidently the CT equation can be justified by our phenomenological approach as well, or it can be derived from a more fundamental perturbative solution to Maxwell's equations. We leave this task to future publications.

We now show how the single scattering results of the Review subsection entitled Single Scattering Photon Correlation Theory may be obtained from the CT equation (Eq. (21)). In a very large weakly scattering medium, that is exposed to steady uniform illumination in a single direction $\mathbf{\Omega}_0$, the correlation function should be time and space independent, yielding a reduced Eq. (21) as

$$G^m(\mathbf{\Omega}, \tau) = S_g(\mathbf{\Omega})/(\sigma + \kappa) + \{\sigma/[4\pi(\sigma + \kappa)]\}\cdot\int_{4\pi} G^m(\mathbf{\Omega}', \tau)g^1(\mathbf{k}', \tau)\Phi(\mathbf{\Omega}, \mathbf{\Omega}')\,d\Omega' \quad (22)$$

where $S_g(\mathbf{\Omega})$ represents the steady illumination in the $\mathbf{\Omega}_0$ direction and can itself be represented in the form

$$S_g(\mathbf{\Omega}) = S_{g0}\delta(\mathbf{\Omega} - \mathbf{\Omega}_0) \quad (23)$$

with S_{g0} being a constant magnitude. A formal solution to this equation is obtained by iteration, and a series in powers of g^1 results. Truncating the series after the first-order term (or performing only one iteration by substituting Eq. (23) for $G^m(\mathbf{\Omega}', \tau)$ into the integral of Eq. (22)) we find

$$G^s(\mathbf{\Omega}, \tau) = S_g(\mathbf{\Omega})/(\sigma + \kappa) + S_{g0}\{\sigma/[4\pi(\sigma + \kappa)^2]\}g^1[\mathbf{k}(\mathbf{\Omega}, \mathbf{\Omega}_0), \tau]\Phi(\mathbf{\Omega}, \mathbf{\Omega}_0) \quad (24)$$

The first term on the right side of Eq. (24) represents the non-attenuated portion of the illumination. The second term represents the single-scattered portion, that is proportional to the single scattering correlation function (g^1) and to the

single particle form factor (cf. Eqs. (6a) and (2c), respectively). Equation (24) demonstrates that Eq. (21) yields the correct single scattering limit of G^m within our stated limitations which neglect polarization.

Approximate Solutions for Small Delay Times

In the following section, we show how DWS theory may be derived from the CT equation. The procedure follows closely those assumptions made to derive the DWS theory.[12] The integral term in Eq. (21) will be approximated by a term containing an integral of only the single scattering correlation function over solid angle. We refer to this approximation as "preaveraging," where the averaging over angles in the single scattering correlation function is disconnected from the propagation/diffusion of the light. The DWS form given in Eq. (12) is derived from this approximate CT equation under the assumptions of small delay times and large optical thickness. Since the CT equation can be reduced to the DWS theory, its solutions should correspond to DWS solutions and give insight into the problems that are encountered in DWS with regard to boundary conditions (i.e., the deposition depth dilemma).

In a following section entitled Reduction of the Time-Independent Correlation Equation, we show how standard RT techniques may be used to solve the approximate CT equation described above for comparison with DWS results. These solutions include both approximate analytical solutions and numerical evaluation of exact solutions. The reader should note that we have assumed isotropic scattering in our derivations such that $l = l^*$ with $\sigma = 1/l$.

Reduction of the Time-Dependent Correlation Transfer Equation

Here we show explicitly how to convert the CT equation given in Eq. (21) from an integro-differential equation to the form of Eq. (12), the DWS form of Ref. 12. First Eq. (21) is written as

$$\frac{(1/c)\partial G^m(\mathbf{r}, \mathbf{\Omega}, t, \tau)}{\partial t} = -\mathbf{\Omega}\cdot\nabla G^m(\mathbf{r}, \mathbf{\Omega}, t, \tau) - \sigma G^m(\mathbf{r}, \mathbf{\Omega}, t, \tau) + (\sigma/4\pi)\int_{4\pi} G^m(\mathbf{r}, \mathbf{\Omega}', t, \tau)\, d\Omega' + (\sigma/4\pi)\int_{4\pi} G^m(\mathbf{r}, \mathbf{\Omega}', t, \tau)[g^1(\mathbf{k}', \tau) - 1]\, d\Omega' + S_g(\mathbf{r}, \mathbf{\Omega}, t) \quad (25)$$

where the integral representing scattering into the $\mathbf{\Omega}$ direction has been written as two integrals, in preparation for "preaveraging" as discussed previously.

In the Ref. 11 formulation, averaging of the singly scattered correlation function (g^1) over all angles is performed before averaging G^m over all paths. We perform a preaveraging approximation for the last integral in Eq. (25) as

$$(\sigma/4\pi)\int_{4\pi} G^m(\mathbf{r}, \mathbf{\Omega}', t, \tau)[g^1(\mathbf{k}', \tau) - 1]\, d\Omega' \approx (\sigma/4\pi)G^m(\mathbf{r}, \mathbf{\Omega}, t, \tau)\int_{4\pi}[g^1(\mathbf{k}', \tau) - 1]\, d\Omega' \approx -\sigma(2\tau/\tau_0)G^m(\mathbf{r}, \mathbf{\Omega}, t, \tau) \quad (26)$$

The approximation of Eq. (6b) has been applied to perform the integral over solid angle. Having invoked Eq. (6b), the final form of Eq. (26) will apply only for $\tau/\tau_0 << 1.0$, such that Eq. (21) becomes

$$\frac{(1/c)\partial G^m(\mathbf{r}, \mathbf{\Omega}, t, \tau)}{\partial t} = -\mathbf{\Omega}\cdot\nabla G^m(\mathbf{r}, \mathbf{\Omega}, t, \tau) - \sigma(1 + 2\tau/\tau_0)G^m(\mathbf{r}, \mathbf{\Omega}, t, \tau) + (\sigma/4\pi)\int_{4\pi} G^m(\mathbf{r}, \mathbf{\Omega}', t, \tau)\, d\Omega' + S_g(\mathbf{r}, \mathbf{\Omega}, t) \quad (27)$$

Fourier tranforming Eq. (27) with $\exp(i\boldsymbol{\omega}\cdot\mathbf{r})$, then Laplace transforming the result with $\exp(-\nu t)$ and solving for the doubly transformed $\tilde{G}^m$ gives

$$\tilde{G}^m(\boldsymbol{\omega}, \Omega, \nu, \tau) = \frac{\tilde{S}(\boldsymbol{\omega}, \mathbf{\Omega}, \nu) + (\sigma/4\pi)\int_{4\pi}\tilde{G}^m(\boldsymbol{\omega}, \mathbf{\Omega}', \nu, \tau)\, d\Omega'}{(\nu/c) + i\boldsymbol{\omega}\cdot\mathbf{\Omega} + \sigma(1 + 2\tau/\tau_0)} \quad (28)$$

In arriving at Eq. (28), it has been assumed that all initial and boundary values of G^m are zero, except that represented by the source S_g. Next, applying the convolution principle to invert Eq. (28) back into the time domain yields

$$W(\boldsymbol{\omega}, \mathbf{\Omega}, t, \tau) = c\int_{-\infty}^{t}\exp[-(i\boldsymbol{\omega}\cdot\mathbf{\Omega}+\sigma)c(t-t')]\cdot\left[V(\boldsymbol{\omega}, \mathbf{\Omega}, t') + (\sigma/4\pi)\int_{4\pi} W(\boldsymbol{\omega}, \mathbf{\Omega}', t', \tau)\, d\Omega'\right] dt' \quad (29)$$

where

$$W(\boldsymbol{\omega}, \mathbf{\Omega}, t, \tau) = \exp(2\sigma c t\tau/\tau_0)\tilde{G}^m(\boldsymbol{\omega}, \mathbf{\Omega}, t, \tau) \quad (30)$$

$$V(\boldsymbol{\omega}, \mathbf{\Omega}, t) = \exp(2\sigma c t\tau/\tau_0)\tilde{S}(\boldsymbol{\omega}, \mathbf{\Omega}, t) \quad (31)$$

If Taylor series expansions in t' about t are substituted for W and V in Eq. (29) and the integrals over t' are performed, the result is

$$W(\boldsymbol{\omega}, \mathbf{\Omega}, t, \tau) = c\int_{-\infty}^{t}\exp[-(i\boldsymbol{\omega}\cdot\mathbf{\Omega}+\sigma)c(t-t')]\cdot\left[\sum_{j=0}^{\infty}\frac{(t-t')^j(-1)^j}{j!}\left(\frac{\partial^j V}{\partial t^j}\right) + (\sigma/4\pi)\cdot\int_{4\pi}\sum_{j=0}^{\infty}\frac{(t-t')^j(-1)^j}{j!}\left(\frac{\partial^j W}{\partial t^j}\right) d\Omega'\right] dt' = \sum_{j=0}^{\infty}\left[\frac{(-1)^j}{c^j(i\boldsymbol{\omega}\cdot\mathbf{\Omega} + \sigma)^{j+1}}\left(\frac{\partial^j V}{\partial t^j} + \frac{\sigma}{4\pi}\int_{4\pi}\frac{\partial^j W}{\partial t^j} d\Omega'\right)\right] \quad (32)$$

where $\partial^0 W/\partial t^0$ is understood to be $W(\boldsymbol{\omega}, \mathbf{\Omega}, t, \tau)$ (with similar notation for V).

Assuming that σc is large and neglecting all terms of order $1/(\sigma c)^2$ and smaller when averaging W and V over all solid angle yields a diffusion equation

$$\frac{\partial\bar{W}(\boldsymbol{\omega}, t, \tau)}{\partial t} = -(c/3\sigma)\omega^2\bar{W}(\boldsymbol{\omega}, t, \tau) + c\bar{V}(\boldsymbol{\omega}, t) \quad (33)$$

where

$$\bar{W}(\boldsymbol{\omega}, t, \tau) = (1/4\pi)\int_{4\pi} W(\boldsymbol{\omega}, \mathbf{\Omega}, t, \tau)\, d\Omega \quad (34)$$

$$\bar{V}(\boldsymbol{\omega}, t) = (1/4\pi) \int_{4\pi} V(\boldsymbol{\omega}, \boldsymbol{\Omega}, t)\, d\Omega \tag{35}$$

Using Green's function to solve Eq. (33), along with the definitions of W and V (Eqs. (30) and (31)), and inverting the Fourier transform variable $\boldsymbol{\omega}$ into real space $\mathbf{r}$, yields

$$\bar{G}^m(\mathbf{r}, t, \tau) = \int_{\text{Vol}} \int_{-\infty}^{t} G(\mathbf{r} - \mathbf{r}', t - t') \cdot \exp[-2\sigma c(\tau/\tau_0)(t-t')]\bar{S}_g(\mathbf{r}, t')c\, dt'\, d^3\mathbf{r} \tag{36}$$

where

$$\bar{G}^m(\mathbf{r}, t, \tau) = (1/4\pi) \int_{4\pi} G^m(\mathbf{r}, \boldsymbol{\Omega}, t, \tau)\, d\Omega \tag{37}$$

$$\bar{S}_g(\mathbf{r}, t) = (1/4\pi) \int_{4\pi} S_g(\mathbf{r}, \boldsymbol{\Omega}, t)\, d\Omega \tag{38}$$

and G is Green's function, which has a form corresponding to the boundary conditions of the problem.

Equation (36) is the result that we wish to compare with Eq. (12). Regrouping terms and changing variables with $t'' = t - t'$ gives

$$\bar{G}^m(\mathbf{r}, t, \tau) = \int_0^{\infty} \exp[-(2\tau/\tau_0)\sigma c t''] \cdot \int_{\text{Vol}} G(\mathbf{r} - \mathbf{r}', t'')\bar{S}_g(\mathbf{r}', t - t'')\, d^3\mathbf{r}' c\, dt'' \tag{39}$$

This is found to be the same form as that of Ref. 10 (Eq. (12)), if the change of variable $s = ct''$ is made in Eq. (39), and the scattering coefficient σ is changed to the form of a mean free path by providing the substitution $\sigma = 1/l$. If we assume a constant source S_g, the second integral over volume is $I_0 J(s)$ as defined in Eq. (11).

Reduction of the Time-Independent Correlation Equation

We will now use the time-independent one-dimensional form of Eq. (27) to determine solutions for backscattering and transmission by radiative transfer methods. Under those assumptions, and setting the source term S_g to zero, Eq. (27) becomes

$$\mu \partial G_1^m(z, \mu, \tau)/\partial z + G_1^m(z, \mu, \tau) = (\tilde{\omega}/2) \int_{-1}^{1} G_1^m(z, \mu', \tau)\, d\mu' \tag{40}$$

where z is the optical coordinate, $z = \sigma(1 + 2\tau/\tau_0)\tilde{z}$, $\tilde{z}$ is the physical coordinate in the z-direction, and $\tilde{\omega}$ is the single scattering albedo, $\tilde{\omega} = 1/(1 + 2\tau/\tau_0)$. In addition, due to the definition of z, the optical thickness of the medium must be $\tilde{L}_e = \tilde{L}(1 + 2\tau/\tau_0) = \tilde{L}/\tilde{\omega}$. Note that G_1^m is the spatially one-dimensional version of G^m.

Equation (40) is a well-known equation in radiative transfer.[27,28] Assuming a collimated boundary condition of $G_1^{m+}(0, \mu, \tau) = G_0^+ \delta(\mu - \mu_0)\delta(\phi - \phi_0)$, the solution for backscattering is[28]

$$G_1^{m-}(0, \mu, \tau; \mu_0) = \frac{[X(\mu)X(\mu_0) - Y(\mu)Y(\mu_0)]}{(\mu + \mu_0)} \frac{G_0^+ \mu_0}{2(1 + 2\tau/\tau_0)} \tag{41a}$$

$$= \frac{G_0^+}{4\mu(1 + 2\tau/\tau_0)} \int_0^{\tilde{L}_e} B(z', \mu_0)\exp(-z'/\mu)\, dz' \tag{41b}$$

and for transmission is

$$G_1^{m+}(\tilde{L}_e, \mu, \tau; \mu_0) = \frac{[X(\mu)Y(\mu_0) - Y(\mu)X(\mu_0)]}{(\mu_0 - \mu)} \frac{G_0^+ \mu_0}{2(1 + 2\tau/\tau_0)} \tag{42a}$$

$$= \frac{G_0^+}{4\mu(1 + 2\tau/\tau_0)} \int_0^{\tilde{L}_e} B(z', \mu_0)\exp[-(\tilde{L}_e - z')/\mu]\, dz' \tag{42b}$$

where the cosine of the incident radiation's angle (μ_0) has been added as a parameter of G_1^m, and X and Y are Chandrasekhar's functions[28]

$$X(\mu) = B(0, \mu) \tag{43}$$

$$Y(\mu) = B(\tilde{L}_e, \mu) \tag{44}$$

with B defined by the integral equation

$$B(z, \mu) = e^{-z/\mu} + (\tilde{\omega}/2) \int_0^{\tilde{L}_e} B(z', \mu)E_1(|z - z'|)\, dz' \tag{45}$$

and the exponential integral being

$$E_1(z) = \int_0^1 \exp(-z/x)\, dx/x \tag{46}$$

In Eqs. (41b) and (42b), G_1^{m-} indicates one-dimensional multiple backscattering, and G_1^{m+} indicates one-dimensional multiple transmission, both dependent on incident angle through μ_0. (Note that Eq. (42b) excludes the non-attenuated portion, of the incident radiation, i.e., the remainder of the original beam.)

Exact solutions for $B(z, \mu)$ are available. But to obtain an analytical trend, an approximate solution for $B(z, \mu)$ can be obtained by the methods employed by Armaly and El-Baz.[29] They approximate the exponential integral by the following:

$$E_1(z) \approx a \exp(-bz) \tag{47}$$

with $a = b = \sqrt{3}$ being the most common choices for the parameters. Substituting Eq. (47) into Eq. (45), and taking the second derivative of the resulting equation with respect to z, yields an ordinary differential equation for B:

$$d^2B(z, \mu)/dz^2 + (\tilde{\omega}ab - b^2)B(z, \mu) = (1/\mu^2 - b^2)\exp(-z/\mu) \tag{48}$$

The solution for B is simply

$$B(z, \mu) = F_1 \exp(-bzR) + F_2 \exp(bzR) + (1/\mu^2 - b^2)\exp(-z/\mu)/[1/\mu^2 - b^2R^2] \tag{49}$$

where $R = (1 - \tilde{\omega}a/b)^{0.5}$ and $\tilde{\omega} \neq b/a$. F_1 and F_2 can be obtained by substituting Eq. (49) back into Eq. (45), evaluating the resulting equation at $z = 0$ and $z = \tilde{L}_e$, then solving for F_1 and F_2. Using this final approximation for $B(z, \mu)$ in Eqs. (41b) and (42b) yields the backscattered and transmitted correlation functions

$$G_1^{m\pm}(z^{\pm}, 1, \tau; \mu_0 = 1) \approx \frac{G_0^+ \tilde{\omega}}{2(1 - R^2b^2)} \left\{ h_1^{\pm} + \left[\frac{\tilde{\omega}b}{(1 - R^2b^2)}\right] \frac{h_2^{\pm} + h_3^{\pm} \sinh(Rb\tilde{L}_e) + h_4^{\mp} \cosh(Rb\tilde{L}_e)}{(2 - \tilde{\omega})\sinh(Rb\tilde{L}_e) + 2R \cosh(Rb\tilde{L}_e)} \right\} \tag{50}$$

where $z^{\pm}$ is either 0 or $\bar{L}_e$, and for $z^{\pm} = 0$

$$h_1^- = (1 - b^2)[1 - \exp(-2\bar{L}_e)]/2$$
$$h_2^- = 2R(b^2 - 1)\exp(-\bar{L}_e)$$
$$h_3^- = (1 + b)(1 - R^2b) + (1 - b)(1 + R^2b)\exp(-2\bar{L}_e)$$
$$h_4^- = R(1 - b^2)[1 + \exp(-2\bar{L}_e)] \quad (51)$$

while for $z^{\pm} = \bar{L}_e$

$$h_1^+ = \bar{L}_e(1 - b^2)\exp(-\bar{L}_e)$$
$$h_2^+ = R(1 + b)^2 + R(1 - b)^2\exp(-2\bar{L}_e)$$
$$h_3^+ = -2(R^2b^2 + 1)\exp(-\bar{L}_e)$$
$$h_4^+ = -2R(1 + b^2)\exp(-\bar{L}_e) \quad (52)$$

When G_1^{m-} and G_1^{m+} are reduced to apply only for short delay time, $(\tau/\tau_0)^{0.5} << 1.0$, and for large optical thickness, $\bar{L}_e >> 1.0$, Eq. (50) becomes

$$G_1^{m\pm}(z^{\pm}, 1, \tau; \mu_0 = 1) \approx \frac{G_0^+(1 - 2\tau/\tau_0)}{2(1 - 6\tau/\tau_0)} \cdot \left[w_1^{\pm} + \frac{\sqrt{3}(1 - 2\tau/\tau_0)}{(1 - 6\tau/\tau_0)} \cdot \frac{w_2^{\pm} + w_3^{\pm}\sinh\left(\bar{L}_e\sqrt{\frac{6\tau}{\tau_0}}\right) + w_4^{\pm}\cosh\left(\bar{L}_e\sqrt{\frac{6\tau}{\tau_0}}\right)}{(1 + 2\tau/\tau_0)\sinh\left(\bar{L}_e\sqrt{\frac{6\tau}{\tau_0}}\right) + 2\sqrt{\frac{2\tau}{\tau_0}}\cosh\left(\bar{L}_e\sqrt{\frac{6\tau}{\tau_0}}\right)} \right] \quad (53)$$

where, for $G_1^{m-}(0, 1, \tau; \mu_0 = 1)$:

$$w_1^- = -1, \qquad w_2^- = 0$$
$$w_3^- = (1 + \sqrt{3})(1 - 2\sqrt{3}\tau/\tau_0)$$
$$w_4^- = -2\sqrt{2\tau/\tau_0} \quad (54)$$

and for $G_1^{m+}(\bar{L}_e, 1, \tau; \mu_0 = 1)$:

$$w_1^+ = w_3^+ = w_4^+ = 0$$
$$w_2^+ = 2(2 + \sqrt{3})\sqrt{2\tau/\tau_0} \quad (55)$$

Equation (53) is similar in functional form and types of arguments to those of Ref. 11 (see Eqs. (14) and (17a)), only the multiplicative constants differ. Thus, as would be expected, the diffusion solution and the optically thick radiative solution yield the same dependence on τ/τ_0.

Discussion

Figure 3 depicts the exact numerical solution of Eq. (41b) for the backscattered correlation function, G_1^{m-}, as a function of the square root of delay time, $(\tau/\tau_0)^{0.5}$, when delay time is near zero. All G_1^{m-} values in Fig. 3 are normalized by the $\bar{L} = \infty$ value of G_1^{m-} at $\tau/\tau_0 = 0.0$. The figure demonstrates a near linear dependence of G_1^{m-} on $(\tau/\tau_0)^{0.5}$ when the optical thickness is infinite. For any finite optical thickness, the small delay time dependence deviates from this behavior. This is the same trend as can be found in the DWS theory of Ref. 12 and results from a reduction in the number of very long multiple scattering paths when the optical thickness is reduced. These very long paths decay most rapidly and contribute most to the initial delay time decay of the correlation function. It is important to note that Fig. 3 shows a near-linear dependence on the square root of delay time at intermediate values of non-dimensional delay time ($0.1 \leq (\tau/\tau_0)^{0.5} \leq 0.2$) for finite thicknesses. This is clearly visible in the region where all of the curves merge. For non-dimensional delay time greater than 0.2, the backscattered correlation function deviates from a linear dependence, that might be expected, given our theoretical restriction to small values of τ from Eq. (26). The linear delay time dependence predicted for small $\bar{L}(\tau/\tau_0)^{0.5}$ in Eq. (18) is examined in Fig. 4 for three optical thicknesses. As the optical thickness ($\bar{L} = L/l$) tends to infinity, $\bar{L}(\tau/\tau_0)^{0.5}$ must tend to zero in order to achieve the Eq. (18) limit. With increasing $\bar{L}$, this limit is realized at decreasingly smaller values of τ/τ_0.

Figure 5 presents the exact transmitted correlation function, g^{m+}, as a function of the non-dimensional delay time (τ/τ_0). In order to compare the trends of g^{m+} for various optical thicknesses, the curves have been scaled such that all zero delay time values ($\tau = 0.0$) are normalized to unity. Examining Fig. 5 reveals that g^{m+} tends to the form given in Eq. (19), for the appropriate limit, which is the small delay time limit of Ref. 12.

Figure 6 presents our exact solution from Eq. (41b) and the Ref. 12 solution from Eq. (15) for infinite optical thickness and for l^* equal to l. The theory of Ref. 12 is parameterized by z_0/l, with z_0/l being a free parameter, because light will not begin diffusing in the sample until it has gone a length of order l. The CT theory does not require knowledge of z_0/l because it accounts for ballistic motion of the photons before diffusion begins. By comparing the exact theory with that given by Ref. 12, we see that z_0/l appears to have a value between 1.21 and 1.33, depending on the range of $(\tau/\tau_0)^{0.5}$, but tending towards 1.33 as τ/τ_0 approaches 0. The Ref. 12

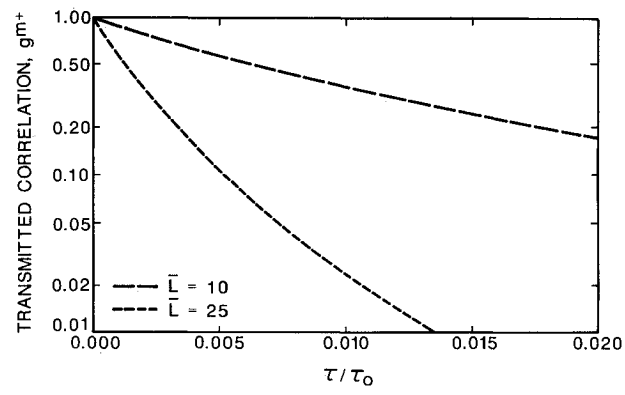

Fig. 5 Comparison of exact transmitted correlation for $\bar{L}$ of 10 and 25.

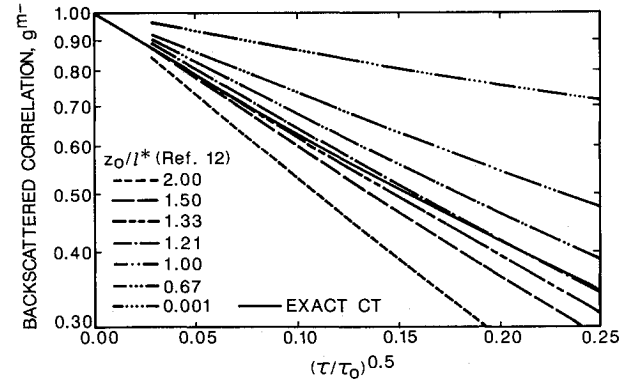

Fig. 6 Comparison of Ref. 12 backscattered correlation with exact for $\bar{L} = \infty$.

comparison of experiment with theory showed that experimental results appear quite linear with $(\tau/\tau_0)^{0.5}$—much more linear than the corresponding theory of theirs or ours. These remarks apply to data in the $(\tau/\tau_0)^{0.5}$ range measured by Ref. 12 (~0.2–0.8). In order to determine z_0/l experimentally, the researchers of Ref. 12 fit the data to the form given by Eq. (16) (i.e., $\exp(-\zeta(\tau/\tau_0)^{0.5})$), assuming that this is the proper small delay time form and that the theory is only valid at small times. Unfortunately, this procedure has produced a number of penetration depth parameters which depend on the details of a given sample, e.g., particle diameter and polarization. At present, it is not clear why the theories deviate from the experimental form for the decay of the correlation function.[30] However, Middleton and Fisher[31] argue that emphasis should be given to the momentum transfer magnitude $(\Sigma_i k_{i,i-1}^2)$ distribution rather than the photon path lengths, as this is the more fundamental variable. Estimates of an approximate distribution function are shown[31] to produce correlation functions having desirable analytic forms. It is not clear from the Ref. 31 work why the DWS theory fails. Alternatively, we give an argument in the Conclusions section that preaveraging leads to the failure of both the approximate CT theory and DWS theory to fit experimental data.

Contrary to the assumption made by Ref. 12, it is unlikely that radiation begins diffusing at a single depth z_0/l. In actuality, the incident radiation is physically deposited, or first scattered, at a distribution of depths. Due to its close relationship to radiative transfer theory, CT theory assumes this distribution implicitly, allowing for the graduated deposition of the incident beam. It seems likely that this deposition distribution has a roughly exponential dependence on depth in the medium. Therefore, if the Ref. 12 equations were multipled by distribution of deposition depths, $\exp(-\beta z_0/l)$, and integrated over z_0/l, the resulting equations would be expected to yield a better match with those of CT theory. Obviously, the suggested exponential distribution is an approximation, and β is unknown. However, if the premise is correct, it should be possible to find a β such that the integrated DWS results more closely match the CT results. Applying the procedure just outlined to Eq. (15) yields the following for backscattered correlation, g^{m-}:

$$g^{m-(\tau)} \propto 1\Big/\left[\left(1+\frac{2}{3}\sqrt{\frac{6\tau}{\tau_0}}\right)\left(\beta+\sqrt{\frac{6\tau}{\tau_0}}\right)\right] \qquad (56)$$

and matching the results to CT theory yields $\beta \cong 0.6$. Figure 7 shows the integrated Ref. 12 results, which have an upward curvature that is even greater than that of the CT theory. However, we also note that the DWS approach makes a continuum approximation in going from Eq. (10) to Eq. (11). This approximation includes single scattering decay ratios smaller than those physically possible when the limit of integration in Eq. (11) extends to zero. This is thought to produce some of the upward curvature in the DWS theory of backscattering at large delay times.[32]

In order to achieve exact agreement between CT theory and integrated DWS, it would be necessary to further investigate the actual deposition distribution involved. The distribution of deposition depths has been previously investigated,[30] but was abandoned because it produced results that did not agree with data as well as the use of a single deposition depth. This is emphasized by the failure of the theories to produce straight lines in Fig. 7 (similar to the Ref. 12 data). Nevertheless, because the approximate CT theory and DWS theory contain the same physics, the proper evaluation of DWS will include some integration over a distribution of deposition depths. Improvement between theory and experiment will be realized only by relaxing one or more of the initial assumptions.

Figures 8 and 9 compare the CT and DWS theories for a finite optical thickness of 10. As was shown in Fig. 3, the

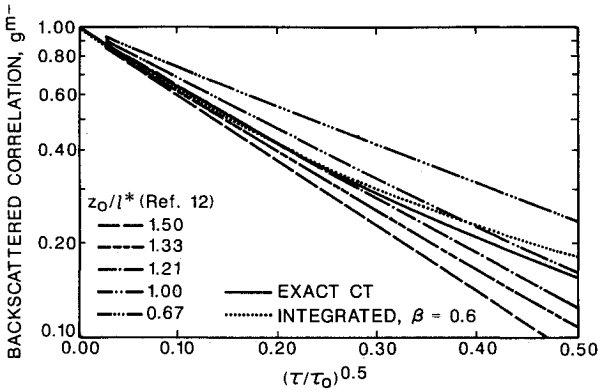

Fig. 7 Comparison of integrated Ref. 12 backscattering with exact for $\bar{L} = \infty$.

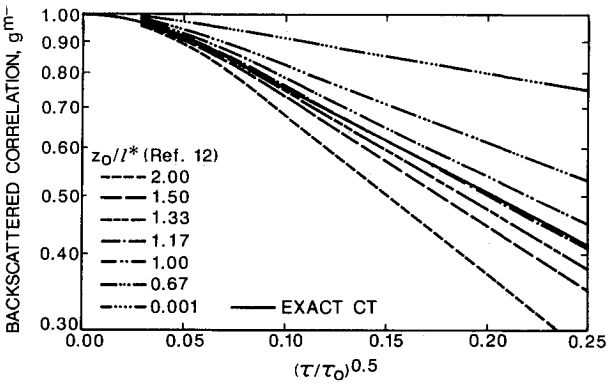

Fig. 8 Comparison of Ref. 12 backscattered correlation with exact for $\bar{L} = 10$.

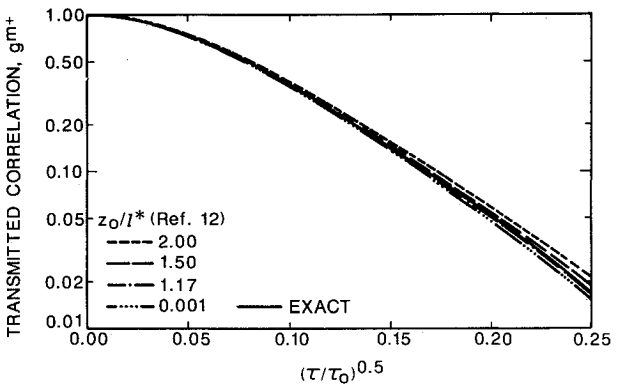

Fig. 9 Comparison of Ref. 12 transmitted correlation with exact for $\bar{L} = 10$.

logarithm of the backscattered correlation does not depend linearly on $(\tau/\tau_0)^{0.5}$ for $(\tau/\tau_0)^{0.5}$ less than 0.1. Even though the curves are not linear in this regime, CT and DWS theories appear to have similar trends. But as with the semi-infinite case, CT theory appears to fit the Ref. 12 theory for a single value of z_0/l equal to 1.33 for small $(\tau/\tau_0)^{0.5}$ and equal to 1.17 for larger $(\tau/\tau_0)^{0.5}$. The finite thickness of the medium appears to have caused that z_0/l value to change from 1.21 to 1.17, when $(\tau/\tau_0)^{0.5} \cong 0.20$. For Figs. 8 and 9, it should be noted that $\bar{L}$ is not significantly larger than z_0/l, as was assumed in the DWS analysis, and could contribute to disagreement between DWS and CT theories. Finally, similar to the integration of the semi-infinite DWS results, we could integrate the finite DWS results over deposition depth, and obtain a better match in the trends of the two theories.

In Fig. 9, transmitted correlation curves show that the match between CT and DWS theories is only good for $(\tau/\tau_0)^{0.5} <$

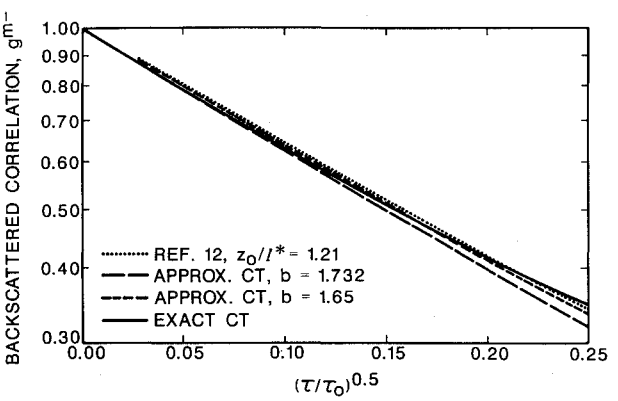

Fig. 10 Comparison of backscattered correlation solutions for $\bar{L} = \infty$.

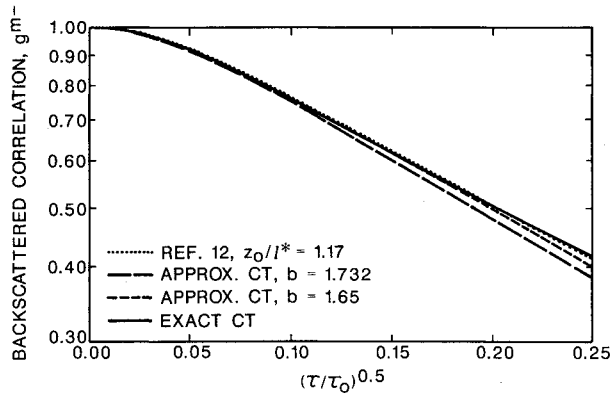

Fig. 11 Comparison of backscattered correlation solutions for $\bar{L} = 10$.

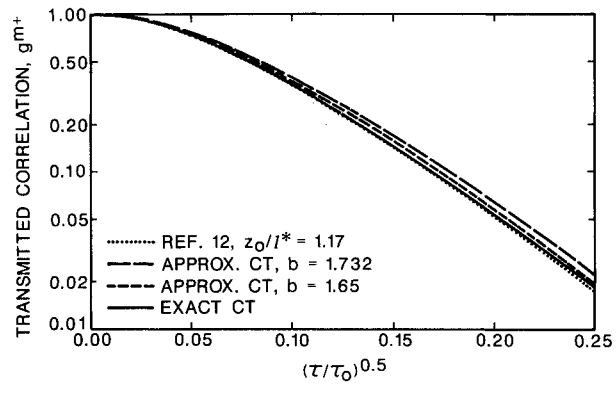

Fig. 12 Comparison of transmitted correlation solutions for $\bar{L} = 10$.

0.1. Figure 9 also demonstrates that z_0/l plays a much smaller role in the DWS theory for transmitted than for backscattered correlation function, that corroborates the form resulting from the reduction of Eq. (17a) to Eq. (17b). Integrating the transmitted DWS result over the exponential distribution of deposition depths produces little change in Fig. 9, provided $\tau/\tau_0 \ll \beta^2/6$. Our examination of that integration (not shown here) indicates that for $\tau/\tau_0 \geq \beta^2/6$, the integrated result becomes nonphysical.

To examine the validity of the approximate CT solutions given by Eqs. (50–55), we compare those solutions with the exact results and with DWS results. Figures 10 and 11 show that the trends of the approximate backscattering solutions are the same as those of the exact solutions for optical thicknesses of infinity and 10, respectively. It appears that the recommended b value, the square root of 3 for Eq. (47), should be replaced by 1.65 for better results in these cases. Figure 12 reinforces this value of b, by showing the comparison of the approximate solution with exact CT and DWS theories for the transmitted correlation function. From these comparisons, we see that the approximate theory can be used in place of the exact theory without significant loss in accuracy. This is advantageous, since the approximate calculation saves considerable computational time as compared to the exact calculation.

Conclusions

We have proposed a CT equation for the description of intensity fluctuations in multiple scattering media. This equation, and the theory behind it, is currently limited to independent scattering with non-polarized light waves. The Fraunhofer limit is also assumed. It has been shown that the CT equation produces the proper single scattering result and can be reduced to the diffusive wave (DWS) theory in the highly multiple scattering limit. Because CT theory is formally similar to RT theory, the techniques applied in this field of study may be applied directly to the CT equation. We have applied such techniques to solve the CT equation in a limit appropriate for DWS. It is implicitly assumed in both DWS and CT theories that the measured intensity correlation is related to the field correlation function in the same way as for single scattering, i.e., by way of the Siegert relationship (cf. Eq. (5a)).

The CT theory accounts for the ballistic nature of light between scattering events and therefore does not suffer from the boundary condition problems encountered in DWS. By comparing the DWS results of Ref. 12 with our CT results for backscattering, we can identify the appropriate deposition length z_0/l needed for DWS theory. This comparison is somewhat artificial because there is actually a distribution of deposition depths. We have investigated an exponential distribution of penetration depths and find a larger upward curvature in the decay of the correlation function, similar to CT results. However, these results yield poorer agreement with experimental data than those produced by using a single deposition depth. Nevertheless, because the approximate CT theory and DWS contain the same physics, the proper evaluation of the DWS will include some integration over a distribution of deposition depths.

We feel that the reason for this disagreement with experimental data is related to the initial assumptions made to produce the DWS results. The experimental data for backscattering from optically dense suspensions produces a correlation function behavior which is linear in the square root of delay time.[12] The DWS and CT theories (in the DWS limit) produce a correlation function showing a slight upward curvature as a function of the square root of the delay time. Thus, these theories produce a slower decay rate at large delay times than that seen experimentally. One obvious criticism of the theories is that they only apply to small delay times $[(\tau/\tau_0)^{0.5} < 0.1]$, and that the experiments exceed the range of validity of the theoretical predictions. However, one may also criticize the preaveraging assumption which averages over all anisotropy in the problem. In particular, the single scattering correlation function given in Eq. (6a) becomes more anisotropic with increasing delay time. Thus, with increasing delay time, the multiple scattering paths contributing to the backscattering, become larger in general. This could lead to a faster decay rate and smaller values for the correlation function with increasing delay time. Preaveraging in DWS or CT (Eq. (26)) does not account for this real effect. However, it is possible to evaluate the CT equation using other approximation schemes. A systematic expansion of the product of the phase function and the single scattering correlation function in the CT equation is possible. A solution which employs the expansion of the anisotropic phase function as a series of Legendre functions would be useful. Keeping only the first term would produce a purely isotropic theory valid for all delay times. We have recently examined such a theory and find it similar to the approximations made for the CT equation

presented here. Initial results of this work indicate improved agreement between theory and experiment. These results will be presented elsewhere.

In this paper, we have limited our investigations to a scalar theory, isotropic scattering, and to independently diffusing Brownian particles. As stated previously, we have found a standard RT approximation which allows us to include anisotropic scattering (l^*) in a natural way and will report on this separately in a later publication. When particle interactions cannot be ignored, the product of the phase function and the single scattering correlation function must be modified to represent the effects of these interactions. If the range of correlation produced by the interactions is sufficiently small, there are many correlation regions in the scattering volume. If, in addition, there is negligible multiple scattering within a correlation region, then the phase function should be modified to include the static structure factor,[2] and the field correlation function should be modified correspondingly. The effect of polarization may be included following the same procedure used in radiative transfer theory,[28] at the expense of making the CT equation more difficult to solve. Other avenues which may prove useful are areas where radiative transfer techniques have produced good analytic approximations. Results for highly anisotropic scattering may be adapted directly to evaluate the CT equation for large particles and/or large delay times. We intend to explore these avenues in future publications and to test our results with appropriate experiments.

Acknowledgments

This work has been supported in part by National Science Foundation, Grant CTS-8907149, and by the Oklahoma Center for the Advancement of Science and Technology, Grants AR9-020 and RE9-003.

References

[1]Berne, B. J., and Pecora, R., *Dynamic Light Scattering,* Wiley, New York, 1976.

[2]Pusey, P. N., and Tough, R. J. A., *Dynamic Light Scattering and Velocimetry: Applications of Photon Correlation Spectroscopy,* edited by R. Pecora, Plenum Press, New York, 1985.

[3]Charalampopoulos, T. T., and Chang, H., "In Situ Optical Properties of Soot Particles in the Wavelength Range from 340 nm to 600 nm," *Combustion Science and Technology,* Vol. 59, 1988, pp. 401–421.

[4]Flower, W. L., "Optical Measurements of Soot Formation in Premixed Flames," *Combustion Science and Technology,* Vol. 33, 1983, pp. 17–33.

[5]Dhont, J. K. G., "Multiple Rayleigh-Gans-Debye Scattering in Colloidal Systems—General Theory and Static Light Scattering," *Physica A,* Vol. 120, 1983, p. 237.

[6]Sorenson, C. M., Mockler, R. C., and O'Sullivan, W. J., "Depolarized Correlation Function of Light Double Scattered from a System of Brownian Particles," *Physical Review A,* Vol. 14, 1976, p. 1520.

[7]Phillies, G. D. J., "Experimental Demonstration of Multiple-Scattering Suppression in Quasielastic-Light-Scattering Spectroscopy by Homodyne Coincidence Techniques," *Physical Review A,* Vol. 24, 1981, p. 1939.

[8]Phillies, G. D. J., "Suppression of Multiple Scattering Effects in Quasielastic Light Scattering by Homodyne Cross-Correlation Techniques," *Journal of Chemical Physics,* Vol. 74, 1981, p. 260.

[9]de Kruif, G. G., Dhont, J. K. G., and Mos, H. J., "Multiple Light Scattering in Colloidal Suspensions: Cross-Correlation Photon Counting Spectroscopy," *Journal de Physique C,* Vol. 3, 1985, p. 149.

[10]Maret, G., and Wolf, P. E., "Multiple Light Scattering from Distorted Media. The Effect of Brownian Motion of Scatterers," *Zeitschrift fuer Physik B,* Vol. 65, 1987, p. 409.

[11]Pine, D. J., Weitz, D. A., Chaikin, P. M., and Herbolzheimer, E., "Diffusing Wave Spectroscopy," *Physics Review Letters,* Vol. 60, 1988, p. 1134.

[12]Pine, D. J., Weitz, D. A., Maret, G., Wolf, P. E., Herbolzheimer, E., and Chaikin, P. M., "Dynamic Correlations of Multiply Scattered Light," *Scattering and Localization of Classical Waves in Random Media,* edited by P. Sheng, World Scientific, Singapore, 1990, pp. 312–372.

[13]Maret, G., and Wolf, P. E., "Weak Localization and Coherent Backscattering of Photons in Disordered Media," *Physics Review Letters,* Vol. 55, 1985, p. 2696.

[14]Von Albada, M. P., and Lagendijk, A., "Observation of Weak Localization of Light in a Random Medium," *Physics Review Letters,* Vol. 55, 1985, p. 2692.

[15]Weitz, D. A., Pine, D. J., Pusey, P. N., and Tough, R. J. A., "Nondiffusive Brownian Motion Studied by Diffusing Wave Spectroscopy," *Physics Review Letters,* Vol. 63, 1989, p. 1747.

[16]Yoo, K. M., Lui, F., and Alfano, R. R., "When Does the Diffusion Approximation Fail to Describe Photon Transport in Random Media?," *Physics Review Letters,* Vol. 64, 1990, p. 2647.

[17]Doob, J. L., "The Browian Movement and Stochastic Equations," edited by N. Wax, *Selected Papers on Noise and Stochastic Processes,* Dover, New York, 1954, pp. 319–337.

[18]Siegel, R., and Howell, J. R., *Thermal Radiation Heat Transfer,* McGraw-Hill, 2nd ed., New York, 1981.

[19]Hiemenz, P. C., *Principles of Colloid and Surface Chemistry,* 2nd ed., Marcel Dekker, New York, 1986, pp. 223–282.

[20]Weiner, B. B., "Particle Sizing Using Photon Correlation Spectroscopy," *Modern Methods of Particle Size Analysis,* edited by H. G. Barth, Wiley, New York, 1984, pp. 93–116.

[21]Siegert, A. J. F., MIT Rad. Lab., Rept. 465, 1943.

[22]Ackerson, B. J., and Clark, N. A., "Dynamic Light Scattering at Low Rates of Shear," *Journal de Physique,* Vol. 42, 1981, p. 929.

[23]Chu, B., *Laser Light Scattering,* Academic Press, New York, 1974.

[24]Ishimaru, A., *Wave Propagation and Scattering in Random Media,* Vol. 2, Academic Press, San Diego, CA, 1978.

[25]Morse, P. M., and Feshbach, H., *Methods of Theoretical Physics,* Vol. II, McGraw-Hill, New York, 1953, p. 1628.

[26]Twersky, V., "Transparency of Pair-Correlated, Random Distributions of Small Scatterers, with Applications to the Cornea," *Journal of the Optical Society of America,* Vol. 65, 1975, p. 524.

[27]Ishimaru, A., *Wave Propagation and Scattering in Random Media,* Vol. 1, Academic Press, San Diego, CA, 1978, p. 204.

[28]Chandrasekhar, S., *Radiative Transfer,* Dover, New York, 1960.

[29]Armaly, B. F., and El-Baz, H. S., "Influence of the Refractive Index on the Radiative Source Function of an Isotropically Scattering Medium," *Journal of Quantitative Spectroscopy and Radiative Transfer,* Vol. 8, 1977, pp. 419–424.

[30]Wolf, P. E., and Maret, G., "Dynamics of Brownian Particles from Strongly Multiple Light Scattering," *Scattering in Volumes and Surfaces,* edited by M. Nieto-Vesperinas and J. C. Dainty, Elsevier Science Publishers, Amsterdam, The Netherlands, 1990, p. 37.

[31]Middleton, A. A., and Fisher, D. S., "Discrete Scatterers and Autocorrelations of Multiply Scattered Light," *Physical Review B,* Vol. 43, 1991, p. 5934.

[32]Pine, D. J., private communication, 1991.